ELSEVIER

Journal of Magnetism and Magnetic Materials 247 (2002) 92–98

journal of magnetism and magnetic materials

www.elsevier.com/locate/jmmm

Particle size effects on magnetic properties of yttrium iron garnets prepared by a sol–gel method

R.D. Sánchez[a,*], J. Rivas[b], P. Vaqueiro[c], M.A. López-Quintela[d], D. Caeiro[b]

[a] *Comisión Nacional de Energía Atómica-Centro Atómico Bariloche and Instituto Balseiro, 8400 Bariloche, Argentina*
[b] *Departamento de Física Aplicada, Facultad de Física, Universidad de Santiago de Compostela, 15782 Santiago de Compostela, Spain*
[c] *Departament of Chemistry, Heriot-Watt University, Riccarton, Edinburgh, UK EH144AS*
[d] *Departamento de Química Física, Facultad de Química, Universidad de Santiago de Compostela, 15782 Santiago de Compostela, Spain*

Received 10 December 2001; received in revised form 13 February 2002

Abstract

We present detailed measurements of field—and temperature—dependence of magnetization in nanocrystalline YIG ($Y_3Fe_5O_{12}$) particles. The fine powders were prepared using sol–gel method. Samples with particle sizes ranging from 45 to 450 nm were obtained. We observe that the saturation magnetization decreases as the particle size is reduced due to enhancement of the surface spin effects. Below a critical diameter $D_s \cong 190$ nm, the particles become single domains and the coercive forces reaches a maximum at diameters close to the critical value. As the particle size decreases the coercivity diminishes and at $D_p \simeq 35$ nm diameters the upper limit of superparamagnetic behavior is reached. A quantitative comparison of temperature and particle size dependence of coercivity shows a satisfactory agreement that is expected for an assembly of randomly oriented particles.

PACS: 75.50.k; 75.60.E; 6146

Keywords: Small particles; Magnetic properties; Yttrium iron garnet

1. Introduction

Nowadays, small magnetic particles have proved to be of great practical use in magnetic recording media, permanent magnets, microwave devices and so on. However, to improve their present applications and develop new uses, a full understanding of their magnetic properties is required. Ferrimagnetic garnets are very well suited for magnetism studies, as these materials have a uniquely defined cation distribution and do not present any site inversion problems which can arise in other ferrites.

In the 1970s, YIG ($Y_3Fe_5O_{12}$) was extensively studied owing to its interesting physical properties. For example, this material was used as a prototype for magnetic studies concerning the dependence of the initial magnetization [1] and the hysteresis loop [2] on the grain size (in the μm region). From these studies a model for the magnetic mechanisms of wall displacement and wall bulging was developed. These days, ferrimagnetic garnets are widely used

*Corresponding author. Tel: +54-2944-445274; fax: +54-2944-445299.
E-mail address: rodo@cab.cnea.gov.ar (R.D. Sánchez).

0304-8853/02/$ - see front matter
PII: S0304-8853(02)00170-1

in electronic devices for the microwave region as well as in magnetic bubble domain-type digital memories [3]. Recently, YIG nanocrystals dispersed on glass have been investigated for high-density magnetic or magneto-optical information storage [4].

In a previous work, YIG particles were synthesized using a low-temperature method based on the citrate gel process. Several modifications of the method were described and the annealing temperature dependence of the magnetic properties was studied for these nanostructured YIG particles [5,6]. This paper is concerned with some of the peculiarities of the magnetic properties of small particles and presents an experimental magnetic study on YIG specimens with a mean particle size in the range 45–450 nm. The critical size for the formation of single-magnetic domain particles in YIG is determined by the size dependence of the coercive field. The dependence of the saturation magnetization on the particle size is also studied.

2. Experimental method

The preparation and characterization of the samples are described in detail elsewhere [5]. Briefly, a gel was obtained from an aqueous solution of citric acid and nitrates of iron(III) and yttrium(III), after heating the solution at 105°C for 2 h. For the preparation of the YIG powders, this gel was dried initially at 105°C for 36 h and further annealing treatments were performed in air at different temperatures (between 400°C and 1000°C) and for different periods of time (between 2 and 24 h). The samples were characterized by X-ray diffraction (XRD) and transmission electron microscopy (TEM). All materials are single phases and exhibit the garnet structure. An expansion of 0.08% was observed in the unit cell parameter of the sample annealed at 800°C. This lattice expansion can be associated with the formation of small amounts of oxygen vacancies [7] and finally, the bulk values were reached smoothly with the increase of the annealing temperature. The mean crystallite size and the microstrains were estimated from XRD measurements [8] with the single line method [9]. This method leads to crystallite sizes slightly lower than those previously reported by us [5], determined using the Scherrer relationship. Crystallite sizes determined from XRD sizes are comparable to those determined from the TEM study and accordingly, one particle contains, on average, one crystallite. Depending on the annealing treatment, we obtained samples with a distribution of the particle sizes, ranging the mean value (and dispersion) from 45 (30) nm to 450 (90) nm.

The magnetic measurements were performed using a vibrating sample magnetometer (VSM) model DMS 1660 with temperature control. Hysteresis loops were recorded up to 10 kOe in the temperature range 77–550 K and also between $H = \pm 2$ kOe at room temperature. Also, we used a SQUID magnetometer in the range of 5–77 K. From each hysteresis loop, we extracted the coercive field (H_c) and the saturation magnetization (M_s). The temperature dependence of the magnetization was measured in the range 300–613 K in an applied field of 100 Oe, after cooling in zero magnetic field (ZFC) or by cooling in a field of 100 Oe (FC).

3. Results and discussion

We shall use the "law of approach to saturation" [10] to describe the isothermal behavior of the saturated magnetization as a function of the size of particles. It is

$$M = M_s\left(1 - \frac{a}{H} - \frac{b}{H^2}\right) + \chi_d H, \tag{1}$$

where a, b and χ_d are constants. The term $\chi_d H$ is the high-field differential susceptibility and represents the field-induced increase in the spontaneous magnetization of the particles. In our case this term, as well as the term that includes the constant a, which is generally interpreted as arising from imperfection effects in the crystals [11], are negligible. A considerable theoretical interest attaches to the b/H^2 term as the constant b is usually identified with the magnetic anisotropy. To study the size effect on the saturation magnetization, M_s values at room temperature were obtained by extrapolation to infinite field in a M

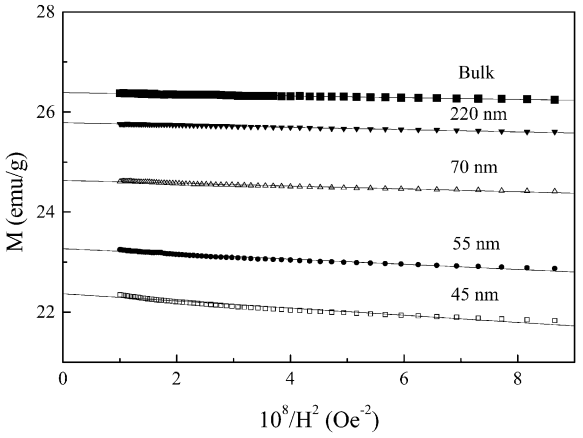

Fig. 1. Dependence of the magnetization on $1/H^2$ at room temperature.

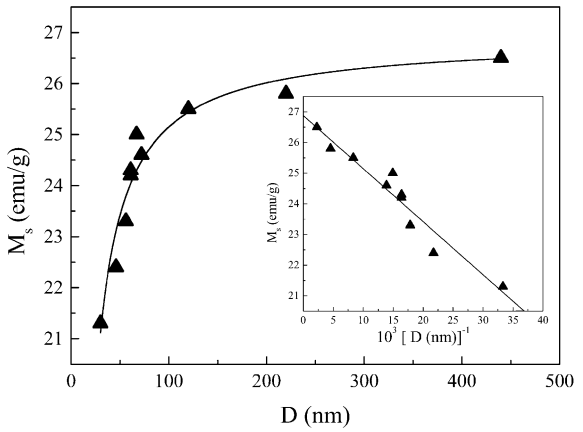

Fig. 2. Variation of the saturation magnetization with the average particle size at room temperature. The inset shows the dependence of the saturation magnetization on the inverse of particle size diameters.

vs. $1/H^2$ plot (see Fig. 1). The saturation magnetization of the particles varies from 21.3 to 26.5 emu/g, and M_s rises with increasing particle size. A similar reduction of the magnetization was observed in small iron [12], γ-Fe_2O_3 [13], $BaFe_{12}O_{19}$ [14], and $MnFe_2O_4$ [15] particles. In Fig. 2, a strong decrease of the saturation magnetization, which occurs for particles smaller than 100 nm, can be observed; a similar behavior has been reported for YIG nanoparticles prepared by a coprecipitation method [16]. This reduction can be related to the higher surface to volume ratio (S/V) in the smaller particles, resulting in a higher contribution from the surface layer. Taking into account that $S/V \sim 1/D$, we plot M_s vs. $1/D$, as illustrated in the inset of Fig. 2. Clearly, the saturation magnetization decreases linearly with the inverse of the particle diameter. This dependence could be expressed as $M_s(D) = M_s(\text{bulk})[1 - \beta/D]$ where $M_s(D)$ is the saturation magnetization of sample with an average diameter D, $M_s(\text{bulk})$ is the bulk saturation magnetization value and β is a constant. From a linear regression analysis of the data presented in the inset of Fig. 2, a value of $M_s(\text{bulk}) = (26.8 \pm 0.2)$ emu/g was obtained, in good agreement with that of the bulk material. Furthermore, for data measured at other temperatures, the saturation magnetization also decreases linearly with the reciprocal of the particle diameter.

This decrease of the saturation magnetization may be attributed to the existence of a non-magnetic surface layer [17] or to a non-collinear spin arrangement at the surface of the particles [18]. However, further experiments would be required in order to determine the degree of spin canting at the surface. If it is assumed that the surface layer has zero magnetization, an approximate value of the layer thickness can be calculated. This procedure leads to a value of the surface layer thickness of ca. 1 nm, which is similar to those reported for the surface layer thickness in other materials.

In Fig. 3, magnetization data for three samples are represented in a plot M_s as a function of $T^{3/2}$ with sizes below and above the critical size in the temperature range 77–300 K. As illustrated by Fig. 3, the temperature dependence of M_s follows a Bloch's $T^{3/2}$ law

$$M = M_s\left(1 - \frac{B}{T^{3/2}}\right), \tag{2}$$

where B is a temperature coefficient which can be derived from Spin-wave theory. As the same that we observe at room temperature above, M_s at zero temperature decreases when the particle size is reduced. The temperature coefficient is expected to

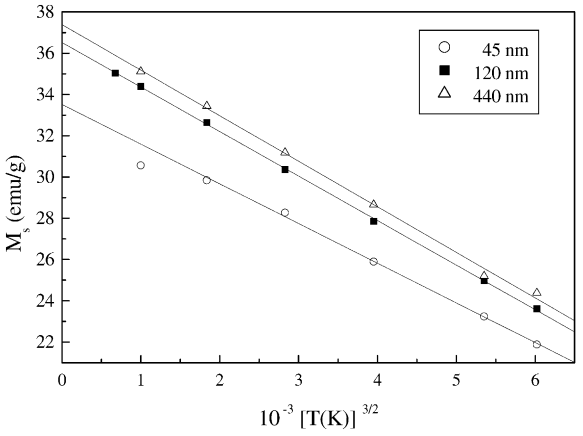

Fig. 3. Temperature dependence of saturation magnetization data. The solid line shows the fit to Bloch's $T^{3/2}$ law.

take the same value for all samples, including the bulk which within the experimental error is the same in Fig. 3.

The temperature dependence of the magnetization after cooling in ZFC and after cooling in a field (FC) are shown in Fig. 4 for three samples in the blocked state region. The following features can be observed in these curves: (1) both curves collapse above a temperature T_s; (2) irreversibilities are observed below T_s, with $M_{ZFC} < M_{FC}$; (3) a maximum value of the ZFC magnetization can be observed at $T_M < T_s$. Although these features could be interpreted as arising from superparamagnetic behavior, the expected Curie like dependence of M vs. T at temperatures between T_s and T_c is absent. Instead a ferromagnetic-like curvature can be observed on approaching the Curie temperature. This behavior could indicate that the system crosses directly the magnetic blocked moment regime to the paramagnetic state.

Other considerations to corroborate the previous point can be found in current theoretical models [19,20] for non-interacting particles. For a given particle size, it is well know that H_c diminishes with increasing temperature. This behavior can be described by the Kneller's formula [21]

$$H_c = H_c^0\left(1 - \sqrt{\frac{T}{T_B}}\right), \tag{3}$$

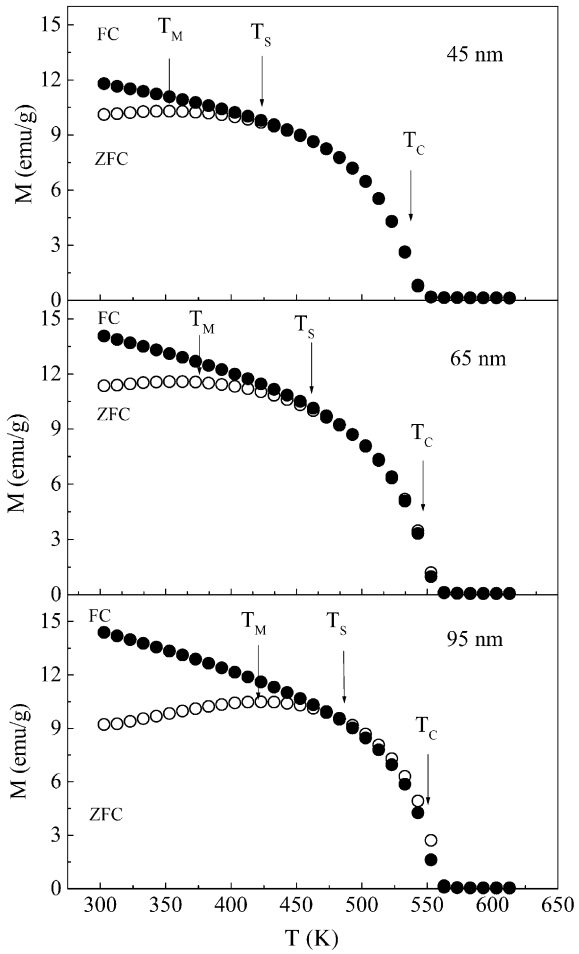

Fig. 4. FC and ZFC magnetization curves measured in a field of 100 Oe for three samples with different sizes in the magnetic moments blocked region.

where the thermal fluctuations of the magnetic moments are being taken into account. For spherical particles, H_c^0 is approximately $2K_1/M_s$, where K_1 represents the anisotropy constant, M_s is the saturation magnetization and T_B is the blocking temperature, which is the upper limit for the temperature region where the magnetic moments of the single-domain particles are blocked. Above this temperature a superparamagnetic behavior is expected. In Fig. 5, we plot H_c vs. $\sqrt{T}$ for a sample with an average particle size of 45 nm, which should lie in the single-domain

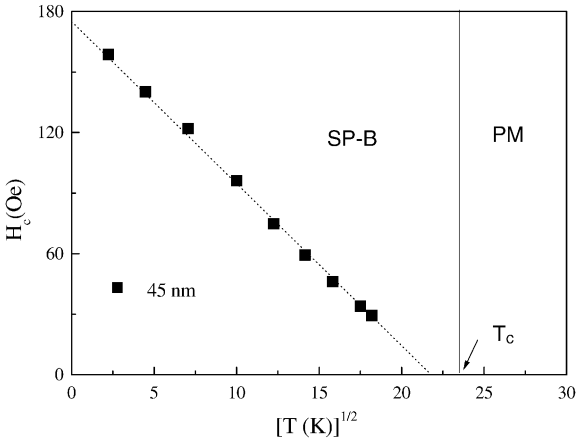

Fig. 5. Coercivity vs. $\sqrt{T}$ for a sample with an average particle size of 45 nm, which is below the critical diameter.

region. A linear behavior is observed, in agreement with Eq. (3). The slope is $H_c^0/\sqrt{T_B} = H_c^0(25k_B/KV)^{1/2}$ and the T_B value depends on the particle volume (V), magnetic anisotropy (K) and the Boltzmann's constant (k_B). Although the slope of H_c vs. $\sqrt{T}$ gives information on the blocking temperature, it can be obtained more easily from the temperature, $T = T_B$, where $H_c = 0$. The T_B value ($\sim 500\,K$), which was estimated from the intercept of the calculated line with the $\sqrt{T}$ axis at $H_c = 0$, is below the Curie temperature ($T_B < T_c$). The coercivity, in the other samples studied, presents a similar thermal behavior to that of the sample described here, but $T_B \approx T_c$. This behavior confirms our previous hypothesis, which was that the magnetic moment of the particles remains blocked up to the Curie temperature. We determined by the extrapolation $\sqrt{T} \to 0$, that H_c^0 is 173(2) Oe for a sample with diameter of 45 nm. Note that the H_c^0 value obtained is the upper limit for smaller particles and a surface contribution or dipolar contribution should be added to the crystal anisotropy fields ($2K_1/M_s = 85$ Oe). Taking $H_c^0 = 2K_{eff}/M_s$ can be calculated the effective anisotropy constant $(1.7 \pm 1) \times 10^4$ erg/cm^3 which includes the extra effects.

At $T = 0\,K$ and for small particle sizes, zero coercive fields are expected owing to superparamagnetic behavior. For diameters larger than D_p, the magnetic moments of the single domain particles are blocked and the coercive field (H_c) exhibits a $D^{-3/2}$ dependence until it reaches a maximum value of H_c^0. This can be expressed by the following equation [21]:

$$H_c = H_c^0\left(1 - \sqrt{\frac{D_p^3}{D^3}}\right). \tag{4}$$

Fig. 6 shows the coercive fields as a function of $D^{-3/2}$ at three temperatures. From the linear portion of these curves, the maximum coercivity fields H_c^0 were obtained by extrapolation to infinite diameters ($D \to \infty$), at each temperature. The values of H_c^0 can be used to normalize the plots of H_c vs. D, because the ratio H_c/H_c^0 is only a function of particle size and not of temperature. A normalized curve of H_c/H_c^0 vs. D, which includes all available data, is plotted in Fig. 7. As illustrated by this figure, the ratio H_c/H_c^0 exhibits a maximum value at a critical size (D_c). This behavior is in good agreement with that expected for small particles and is related to the existence of different magnetic processes in the particles. For single domain particles ($D < D_c$), the size dependence of the normalized coercivity can be described by Eq. (4). The upper limit of the particle diameter for superparamagnetic behavior can be estimated by fitting the data plotted in Fig. 7 with

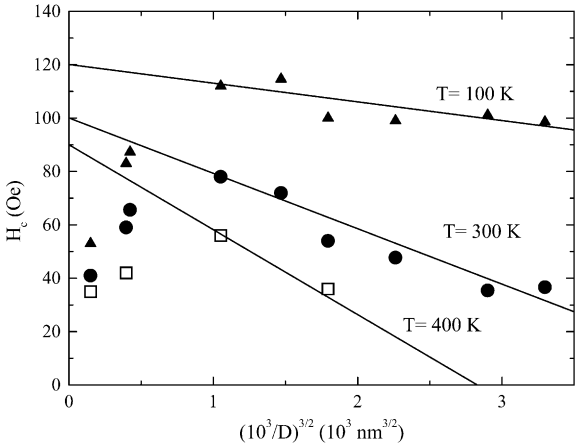

Fig. 6. Coercivity measured at different temperatures, 100, 300 and 400 K for different average particle sizes as a function of $D^{-3/2}$.

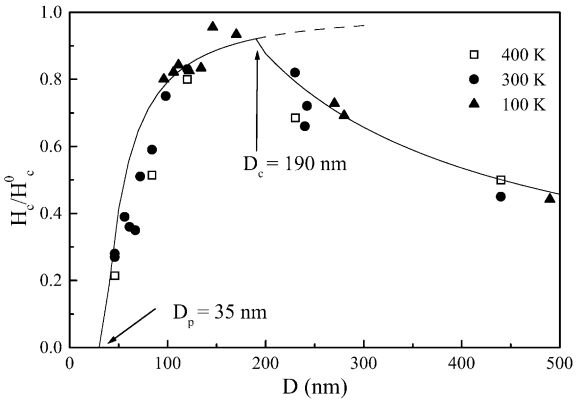

Fig. 7. Normalized coercivity (H_c/H_c^0) as a function of the average particle size (D). Solid lines show the behavior predicted for an assembly of small particles.

Eq. (4). A value of $D_p \simeq 35\,\text{nm}$ was obtained. Above D_c, the changes in behavior are caused by the formation of nucleation centres in which incoherent rotations of the magnetization are expected to take place [6,22]. The formation of walls between magnetic domains takes place at a critical particle size for single-magnetic domain behavior D_s being normally $D_s > D_c$. Experimentally we found that the coercivity follows a $D^{-\alpha}$ dependence with $\alpha = 0.71(1)$ for $D > D_c$ (see solid line in Fig. 7).

The critical particle size below which a spherical particle will be single domain in zero applied field, can be estimated by the following equation [22]:

$$D_s = \frac{9}{2\pi}\left(\frac{\gamma}{M_s^2}\right) \tag{5}$$

where γ is the wall energy and M_s is the saturation magnetization. The wall energy was calculated as $\gamma = 4\sqrt{AK_1}$ where A is the exchange constant and K_1 the anisotropy constant. The exchange constant A can be calculated with the relationship $A(T) = k_B T_c/a\sqrt{1 - T/T_c}$, where T_c is the Curie temperature and a is the lattice parameter. The following values have been taken from the literature [23]: the lattice parameter ($a = 12.376 \times 10^{-8}\,\text{cm}$), the Curie temperature ($T_c = 550\,\text{K}$) and the anisotropy constant ($K_1 = 6.1 \times 10^3\,\text{erg/cm}^3$) and then we have calculated the critical diameter value $D_s \sim 190\,\text{nm}$, using Eq. (5). Although it has been reported that this expression provides not very accurate estimates [24], our calculated value using Eq. (5) agrees with previous estimates [1] which suggest that the critical single-domain diameter should be $< 0.2\,\mu\text{m}$ for the YIG material. Note that this coincidence of the crossover diameter for nucleation processes and the critical diameter for domain formation is not generally observed in other materials. Also, we can calculate the wall thickness δ_W; for this low anisotropy material we can calculate the wall thickness, $\delta_W = \sqrt{A/K_1}$, which is of the order of 80 nm.

Important shape effects are not expected in the quasi-spherical YIG particles. By other way, the presence of exchange interaction between neighboring particles also is discarded because the magnetic cores are insolated by the dead magnetic surface layer and the magnetic moments between the particles are un-coupled. In the best of the case and considering a compacted powder, these cores should be separated by 20 Å. At least, the direct exchange needs 4 Å while the superexchange interaction 8 Å for switch on the interaction. By these reasons, this interaction between the particles is practically negligible. However, the dipolar fields can affect the magnetic properties as the coercive field but these only introduce a bias. For a fanning configuration of the moments, the coercive force ($H_c = \pi M_s/6$) [25] is estimated in approximately 75 Oe. It can explain the H_c^0 value obtained at low temperature by extrapolation in Fig. 5. As we normalized H_c (see Figs. 6 and 7), the influence of the dipolar interaction is canceled and the shift of the coercive field does not invalid the conclusions arrived in the paper.

Another aspect to discuss is the ferromagnetic-like behavior of M observed in Fig. 4, which may be influenced by the dipolar interaction shifting the blocking temperature to higher values (near of T_c). But also, it is reasonable to think, that the system has a lognormal distribution [26] of particle volume (or T_B) contributing with an important fraction of particles with larger sizes. These sizes give blocking temperatures near T_c with the ferromagnetic-like behavior observed.

4. Conclusions

In conclusion, we have studied the magnetic properties of YIG nanoparticles, with sizes between 45 and 450 nm, prepared using a sol–gel method. We have presented a normalized coercivity curve which demonstrates that the dependence of the magnetic properties on particle size follows the behavior expected for a system of small particles. In this study, we have determined an upper limit for the particle size for superparamagnetic behavior of 35 nm and the critical size of 190 nm, at which the single-magnetic domains begin to appear. The non-collinearity of the spins at the surface of the particles is manifested in the size dependence of the saturation magnetization values.

Acknowledgements

The authors wish to acknowledge Dr. D. Fiorani for useful discussion. One of the authors (R.D.S) gratefully acknowledges financial support of CONICET (Argentina).

References

[1] A. Globus, P. Duplex, M. Guyot, IEEE Trans. Magn. 7 (1971) 617.
[2] A. Globus, M. Guyot, Phys. Stat. Sol B 52 (1972) 427.
[3] M.A. Gilleo, Ferromagnetic Materials: A Handbook of the Properties of Magnetically Ordered Substances, E.P. Wohlfarth, (Ed.), North-Holland, Amsterdam, Vol. 2, 1980 (Chapter 1).
[4] S. Taketomi, C.M. Sorensen, K.J. Kabunde, J. Magn. Magn. Mater. 222 (2000) 54.
[5] P. Vaqueiro, M.P. Crosnier-Lopez, A. López-Quintela, J. Solid State Chem. 126 (1996) 161.
[6] P. Vaqueiro, M.A. López-Quintela, J. Rivas, J.M. Greneche, J. Magn. Magn. Mater. 169 (1997) 56.
[7] R. Metselaar, M.A.H. Huyberts, J. Phys. Chem. Solids 34 (1973) 2257.
[8] P. Vaqueiro, M.A. López-Quintela, Chem. Mater. 9 (1997) 2836.
[9] Th.H. De Keijser, J.L. Langford, E.J. Mittemeijer, A.B.P. Vogels, J. Appl. Crystallogr. 15 (1982) 308.
[10] A.H. Morrish, The Physical Principles of Magnetism, IEEE Press, New York, 2001;
A. Herpin, Theorie du Magnetisme, Presses Universitaries de France, Paris, 1968.
[11] L. Néel, J. Phys 9 (1948) 193.
[12] S. Gangopadhyay, G.C. Hadjipanayis, B. Dale, C.M. Sorensen, K.J. Klabunde, V. Papaefthymiou, A. Kostikas, Phys. Rev. B 45 (1992) 9778.
[13] D.H. Han, J.P. Wang, H.L. Luo, J. Magn. Magn. Mater. 136 (1994) 176.
[14] X. Batlle, X. Obradors, M. Medarde, J. Rodríguez-Carvajal, M. Pernet, M. Vallet-Regí, J. Magn. Magn. Mater. 124 (1993) 228.
[15] Z.X. Tang, C.M. Sorensen, K.L. Klabunde, G.C. Hadjipanayis, Phys. Rev. Lett. 67 (1991) 3602.
[16] K. Haneda, A.H. Morrish, Nucl. Instrum. Methods. in Phys. Res. B 76 (1993) 132.
[17] A.E. Berkowitz, W.J. Schuele, P.J. Flanders, J. Appl. Phys. 39 (1968) 1261.
[18] A.H. Morrish, K. Haneda, J. Phys. Colloq. 41 (1980) C1–171.
[19] J.L. Dorman, D. Fiorani, E. Tronc, Magnetic relaxation in fine particle system, in: I. Prigogine, S.A. Rice (Eds.), Advances in Chemical Physics, Vol. XCVIII, Wiley, New York, 1997.
[20] C.L. Chien, J. Appl. Phys. 69 (1991) 5267.
[21] E.F. Kneller, F.E. Luborsky, J. Appl. Phys. 34 (1963) 656.
[22] H. Kronmüller, in: G.J. Long, F. Grandjean (Eds.), Supermagnets Hard Magnetic Materials, Kluwer, Dordrecht, 1991, p. 461.
[23] Landolt-Börnstein, Numerical Data and Functional Relationships in Science and Technology Series III, Vol. 12a, Springer, Berlin, 1996.
[24] A. Aharoni, IEEE Trans. Magn. MAG-22 (1986) 478.
[25] B.D. Cullity, in: M. Cohen (Ed.), Introduction to Magnetic Materials, Addison-Wesley, Reading, MA, 1972.
[26] X. Batlle, M. García del Muro, J. Tejada, H. Pfeiffer, P. Görnet, E. Sinn, J. Appl. Phys. 74 (1993) 3333.